Developmental basis of sexually dimorphic digit ratios

Zhengui Zheng and Martin J. Cohn[1]

Howard Hughes Medical Institute and Department of Molecular Genetics and Microbiology and Department of Biology, University of Florida, Gainesville, FL 32610

Males and females generally have different finger proportions. In males, digit 2 is shorter than digit 4, but in females digit 2 is the same length or longer than digit 4. The second- to fourth-digit (2D:4D) ratio correlates with numerous sexually dimorphic behavioral and physiological conditions. Although correlational studies suggest that digit ratios reflect prenatal exposure to androgen, the developmental mechanism underlying sexually dimorphic digit development remains unknown. Here we report that the 2D:4D ratio in mice is controlled by the balance of androgen to estrogen signaling during a narrow window of digit development. Androgen receptor (AR) and estrogen receptor α (ER-α) activity is higher in digit 4 than in digit 2. Inactivation of AR decreases growth of digit 4, which causes a higher 2D:4D ratio, whereas inactivation of ER-α increases growth of digit 4, which leads to a lower 2D:4D ratio. We also show that addition of androgen has the same effect as inactivation of ER and that addition of estrogen mimics the reduction of AR. Androgen and estrogen differentially regulate the network of genes that controls chondrocyte proliferation, leading to differential growth of digit 4 in males and females. These studies identify previously undescribed molecular dimorphisms between male and female limb buds and provide experimental evidence that the digit ratio is a lifelong signature of prenatal hormonal exposure. Our results also suggest that the 2D:4D ratio can serve as an indicator of disrupted endocrine signaling during early development, which may aid in the identification of fetal origins of adult diseases.

limb development | sexual dimorphism | steroid hormones

In human hands, the relative lengths of the second and fourth fingers differ between males and females. In males, the second digit (2D, or index finger) is usually shorter than the fourth digit (4D, or ring finger), whereas in females the index finger is generally equal to or longer than the ring finger (Fig. 1A). The ratio of 2D length to 4D length, known as the 2D:4D ratio, is therefore 2D:4D < 1 for most men and 2D:4D ≥ 1 for most women. This sexually dimorphic character of the limb was described >120 y ago (1), but it was not until 1998 that the 2D:4D ratio was linked to sex steroids by the observation that men with lower 2D:4D ratios have higher serum testosterone and lower estrogen levels (2). The discovery that sexually dimorphic digit ratios exist in 2-y-old children raised the possibility that 2D:4D ratios are determined early in life (2). These studies led to the hypothesis that a low 2D:4D ratio reflects embryonic exposure to high levels of testosterone, whereas a high 2D:4D ratio reflects a prenatal environment low in testosterone (3). This hypothesis has not been tested experimentally.

There has been increasing use of the 2D:4D ratio as an index of prenatal hormone exposure, and extensive studies in humans have found correlations between digit ratios and a variety of physiological and psychological conditions, including fertility (4), athletic ability (5), sex-biased diseases (6, 7), social behaviors (3, 8), and sexual orientation (9). Most of the evidence linking digit ratios to differences in androgen and estrogen during development is indirect and based on correlational studies in humans after birth (10, 11). It remains unknown whether prenatal androgen and estrogen play causal roles in sexual dimorphism of the digit ratios and how these sex steroids could influence the mechanisms of digit development. In this study, we show that sexually dimorphic

2D:4D ratios in mice are similar to those of humans and are controlled by the relative levels of androgen to estrogen signaling in utero. These findings indicate that the 2D:4D ratio is determined by (and is a reflection of) the hormonal milieu at the time of digit cartilage development and provide experimental validation for the use of digit ratios as an index of the uterine environment, which has implications for interpreting the developmental basis of sexual dimorphism, behavior, and disease.

Results

Sexually Dimorphic Digit Development in Mice. To determine the developmental basis of the sexually dimorphic 2D:4D ratio, we first confirmed that sexual dimorphism exists in the CD-1 mouse strain, as previous studies of mouse digit ratios have reached different conclusions that may reflect strain differences (12–15). Forelimbs and hindlimbs of CD-1 mice showed sexually dimorphic digit ratios, with hindlimb digits showing the greatest similarity to the proportions of human hands (Fig. 1). Therefore, all subsequent analyses were performed on mouse hindlimbs. Morphometric analysis of 58 CD-1 mouse skeletons (30 males and 28 females) at postnatal day (P) 21 revealed that male and female 2D:4D ratios are significantly different; in the right hindlimb, for example, males have a mean 2D:4D ratio of 0.984, and females have a mean ratio of 1.006 ($P = 0.034$; Fig. 1 B and C).

Humans show sexual differences in the 2D:4D ratio as early as 2 y of age, although it is unknown whether this difference arises during prenatal limb development or postnatal growth (2). To determine whether digit length is specified differently in male and female mice, we used expression of Sox9, the earliest molecular marker of cartilage differentiation, to label the primordium of each digit and then measured the length of the Sox9 domain in the second and fourth rays (Fig. 1D). At embryonic day (E) 12.5, when cartilage condensations first appear, 2D < 4D, and the ratio was not significantly different between males and females ($P = 0.687$; Fig. 1E), indicating that the sexual dimorphism arises after condensation of the digit primordia. By E17, however, a small but significant sexually dimorphic 2D:4D ratio had emerged in the right hind paw; the male mean 2D:4D ratio was 0.962, but the female mean ratio was 0.981 ($P = 0.013$; Fig. 1 F and G). Interestingly, the left hind paw showed no significant difference between males and females ($P = 0.068$; Fig. 1G), which is similar to the left–right asymmetry that exists in adult humans; however, in mice, both left and right hind paws exhibited a significant dimorphism by P21 (Fig. 1C). These results indicate that the sexually dimorphic 2D:4D ratio in mice develops during a narrow window of embryonic development—after formation of the digit condensations but before E17—and does not change postnatally (Fig. 1 B, C, F, and G).

Differential Distribution of Androgen and Estrogen Receptors in Digits. Androgen receptors (ARs) and estrogen receptors (ERs)
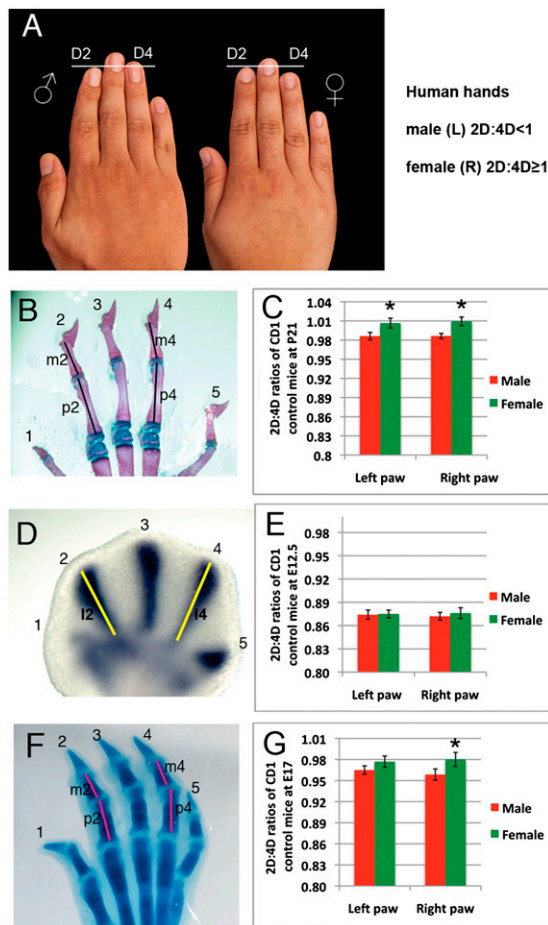
Fig. 1. Ontogeny of the 2D:4D ratio. (*A*) Male (*Left*) and female (*Right*) adult human hands showing dimorphic 2D:4D ratios. Horizontal line marks the distal tip of the second digit (D2). Note that the fourth digit (D4) is longer than 2D in the male but shorter than 2D in the female. (*B*) Mouse foot skeleton at postnatal day (P) 21. Digits are numbered, and vertical lines show axes of measurement for proximal (p) and middle (m) phalanges of 2D and 4D. (*C*) The mean 2D:4D ratio at P21 is smaller in males (*n* = 30) than in females (*n* = 28). (*D*) Whole-mount in situ hybridization showing *Sox9* mRNA (purple stain), which marks the precartilagenous condensations, in right footplate at embryonic day (E) 12.5. Yellow lines show axes measured. (*E*) The mean 2D:4D ratio is the same for males (*n* = 21) and females (*n* = 19) at E12.5. (*F*) E17 mouse right foot stained with alcian blue to show cartilage. (*G*) The mean 2D:4D ratio in E17 males (*n* = 18) is significantly smaller than females (*n* = 22) in right hind paws. Error bars show ± SEM. *P < 0.05.

mediate the activities of androgens and estrogen, respectively, and are activated when ligand binding occurs in the cytoplasm, which induces translocation of the ligand–receptor complexes into the nucleus, where they function primarily as transcription factors that bind DNA and regulate gene expression (16, 17). We asked whether AR and ER proteins are present in the developing digits before and during sexually dimorphic development. In E12.5 males and females, ∼90% of the cells in developing digits were AR-positive (Fig. 2 *A–D*), with 80% of the cells showing nuclear localization and only 10% showing cytoplasmic localization of AR (Fig. 2*D*), suggesting that AR is active in most cells at the time of cartilage condensation. Comparison of 2D and 4D showed that nuclear localization of AR was significantly higher in 4D in both males (*P* = 0.027) and females (*P* = 0.039; Fig. 2*D*).

By E14.5, males and females showed differences in the nuclear localization of AR in 4D, with >95% of the cells staining positive in the male 4D, compared with 70% of the cells in the female 4D (Fig. 2 *E–H*). Thus, between E12.5 and 14.5, AR activity in 4D increased in males but decreased in females. In both sexes, nuclear AR

remained more abundant in 4D than in 2D (*P* = 0.013 for males and 0.022 for females), suggesting that androgen signaling was higher posteriorly.

Variation of 2D:4D ratios is widely considered to reflect different prenatal androgen levels, although it also has been reported that estrogen levels correlate positively with 2D:4D ratios (2, 11, 18). To determine whether estrogen signaling could have a role in the regulation of digit proportions, we investigated ER-α distribution during digit development. ER-α protein was present in the developing digits of both sexes at E12.5, 14.5, and 16.5 (Fig. 2 *I–P* and Fig. S1 *D–G*). At E12.5, most (85%) of the cells in the digit condensations were ER-α–positive (Fig. 2 *I–L*), and, as with AR, we detected significantly more ER-α–positive cells in 4D than 2D in males (*P* = 0.022) and females (*P* = 0.025; Fig. 2*L*). A notable contrast between ER-α and AR distribution is that, in both sexes, only 10% of ER-α–positive cells showed nuclear localization of the protein at E12.5, suggesting that most ER-α was inactive at this stage, and we observed no significant difference between 2D and 4D (*P* = 0.568 for males and 0.186 for females; Fig. 2 *K* and *L*). By E14.5, however, ER-α had become predominantly nuclear in the digit condensations of both sexes and, like AR, was more abundant in 4D than 2D (*P* = 0.0159 for males and 0.0264 for females; Fig. 2 *M–P*). These patterns indicate that ER-α is active in the digits between E12.5 and 14.5 and that estrogen signaling is stronger in 4D of both sexes.

In males and females at E16.5, both AR and ER-α were weaker in the proliferative zones, but ER-α remained strong in the hypertrophic zone of the proximal phalanx (Fig. S1 *A–F*). Interestingly, at this stage, we found no significant differences in the number of ER-α–expressing cells in 2D and 4D of both sexes (Fig. S1*G*). The results suggest that ER-α may play a role in chondrocyte hypertrophy and elongation, but the lack of a difference between 2D and 4D at this stage supports the hypothesis that sexually dimorphic digit development is established before E16.5.

Given that activated AR and ER-α were more abundant in 4D of males and females by E14.5, we asked whether levels of activated receptor in 2D relative to 4D differed between the sexes. The difference in AR activity between 2D and 4D ($\Delta AR = AR^{4D} - AR^{2D}$) was greater in males (*P* = 0.025; Fig. 2*H*), whereas the 2D:4D difference in ER-α activity ($\Delta ER\text{-}\alpha = ER\text{-}\alpha^{4D} - ER\text{-}\alpha^{2D}$) was greater in females (*P* = 0.008; Fig. 2*P*). The finding that males had a higher ΔAR and females had a higher ΔER raises the possibility that it is the relative difference in androgen vs. estrogen activity (rather than absolute levels of either) that underlies sexually dimorphic 2D:4D ratios.

AR and ER also can have nongenomic modes of action, in which they signal through the mitogen-activated protein kinase (MAPK)/ERK pathway (19, 20). To determine whether these receptors activate nongenomic signaling in the digits, we monitored the mRNA levels of Mapk1 and Mapk3 in 2D and 4D. We found no significant differences in *Mapk1* and *Mapk3* expression between male, female, and flutamide-treated male digits at E14.5, suggesting that nongenomic signaling plays little (if any) role in sexual dimorphism of digits (Fig. S2).

Modulation of Androgen and Estrogen Signaling Alters Digit Ratios.
Based on our discoveries that mouse toes mimic the sexually dimorphic digit ratios found in human fingers and that AR and ER-α show different 2D:4D patterns in male and female mice, we deleted AR and ER-α to test directly the hypothesis that prenatal androgen and estrogen signaling underlies sexually dimorphic digit development. When AR was deleted in the limb (using *Prx1^Cre*; ref. 21), mutant males showed significantly increased 2D:4D ratios over those of control mice, which expressed *Cre* but were wild type for AR (*P* = 0.021; Fig. 3*A*). We then examined the effects of deleting ER-α and found that homozygous mutant males developed decreased 2D:4D ratios relative to controls (*P* = 0.049; Fig. 3*A*). Thus, AR and ER have opposite effects on the digit ratio; AR is necessary for development of a masculine/low 2D:4D ratio, whereas ER-α is required for development of a feminine/high 2D:4D ratio.
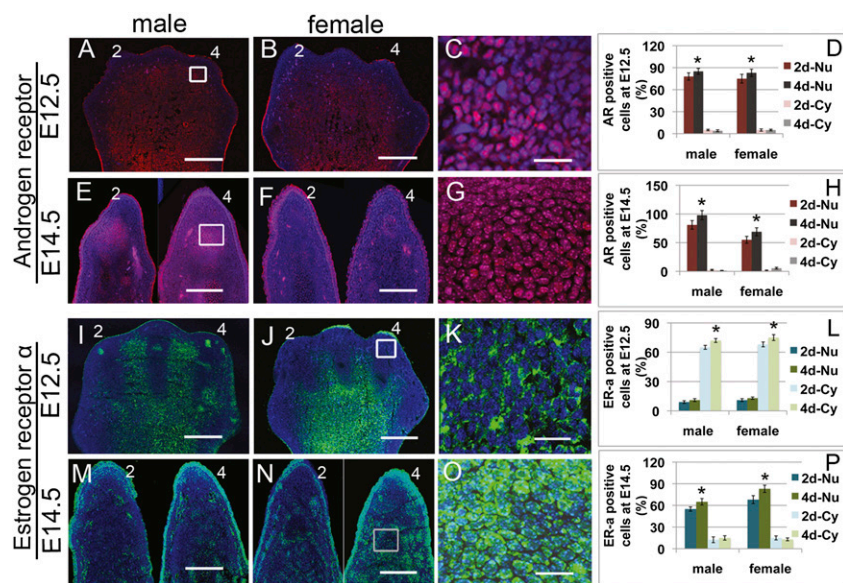
Fig. 2. AR and ER-α distribution in developing digits. (*A–C, E–G, I–K,* and *M–O*) Immunolocalization of AR (red, *A–C* and *E–G*) and ER-α (green, *I–K* and *M–O*) in mouse digits at E12.5 and 14.5. Blue signal is DAPI. Stage is indicated at left, sex is indicated at top, and 2D and 4D are numbered. White boxes in *A, E, J,* and *N* are shown at high magnification in *C, G, K,* and *O,* respectively. (*D, H, L,* and *P*) Quantitative analysis of AR-positive (*D* and *H*) and ER-α–positive (*L* and *P*) cells with nuclear (Nu) and cytoplasmic (Cy) staining. Note that 4D has the highest levels of activated (nuclear) AR in males and females at E12.5 (*C* and *D*) and E14.5 (*G* and *H*), although levels drop in the female between these stages. ER-α staining is also higher in 4D at both stages (*L* and *P*). ER-α is mostly cytoplasmic at E12.5 (*K* and *L*), but by E14.5, most of the ER-α has gone to the nucleus (*O* and *P*). Error bars show ± SEM. *$P <$ 0.05. (Scale bars: 100 μm, *A, B, I,* and *J*; 30 μm, *E, F, M,* and *N*; 10 μm, *C, G, K,* and *O*.)

To identify the temporal window of sensitivity to androgen and estrogen signaling, we administered receptor antagonists or ligands to pregnant females between stages E12.5 and 15.5. Treatment of pregnant females with flutamide (120 mg/kg), a pharmaceutical antiandrogen that specifically binds and inactivates AR (22), between E12.5 and 15.5 caused male offspring to develop higher/feminized 2D:4D ratios (2D:4D = 1.024 vs. 0.987 in controls; $P =$ 0.021; Fig. 3*B*). When pregnant females were given dihydrotestosterone (DHT; 2 mg/kg) during the same developmental window, female offspring had lower/masculinized 2D:4D ratios (2D:4D = 0.992 vs. 1.008 in controls; $P =$ 0.033; Fig. 3*B*). Digit development was unaffected by treatment with the corn oil vehicle alone. Thus, a prenatal environment high in androgen induces development of a 2D:4D ratio <1. To determine whether modulation of prenatal estrogen could influence sexual dimorphism of the digits, pregnant females were treated with estradiol (300 μg/kg) from E12.5 to 15.5, which significantly increased/feminized the 2D:4D ratios in male offspring (2D:4D = 1.016 vs. 0.987 in controls; $P =$ 0.019; Fig. 3*B*).

We also tested whether postnatal modulation of androgen and estrogen signaling affects digit ratio. Treatments with flutamide, DHT, and estradiol at P0–3 failed to induce significant changes of 2D:4D ratios when measured at P21 (Fig. 3*B*), although the anogenital distance was reduced significantly in flutamide-treated ($P =$ 0.001) and estradiol-treated ($P =$ 0.005) mice (Fig. S3). These results demonstrate that 2D:4D ratios are influenced by prenatal, but not by early postnatal, hormonal activity. Thus, although anogenital distance reflects both prenatal and postnatal effects of sex steroids, 2D:4D ratio is a readout of prenatal sex steroid activity only.

We next investigated how early the digit proportions could be influenced by sex steroids. We antagonized AR and ER from E12.5 to 15.5 and then measured the length of the digit cartilages 36 h later, at E17. Male embryos in which AR activity was antagonized with flutamide exhibited increased/feminized 2D:4D ratios at E17 (2D:4D = 1.009 vs. 0.963 in controls; $P =$ 0.009), and females exposed to an ER antagonist (fulvestrant, 1 mg/kg) displayed decreased/masculinized 2D:4D ratios (2D:4D = 0.944 vs. 0.981 in controls; $P =$ 0.008; Fig. 3*C*). ER antagonism also decreased the 2D:4D ratio in males, effectively hypermasculinizing their digit proportions (Fig. S4). We also tested the effects of increasing androgen or estrogen levels at E12.5–15.5 and found that as early as E17, males exposed to estradiol showed increased 2D:4D ratios (2D:4D = 1.004; $P =$ 0.013), and females exposed to DHT showed decreased 2D:4D ratios (2D:4D = 0.957; $P =$ 0.016; Fig. 3*C*). Together with the finding that AR and ER are active at higher

levels in 4D than in 2D in both sexes at E14.5 (Fig. 2), these data indicate that sexually dimorphic digit proportions are caused by prenatal differences in androgen and estrogen signaling. Interestingly, previous studies of human fetuses reported that by wk 14, the digit proportions resemble those of adults (23), which is consistent with the findings of an independent study that showed little change in digit dimorphism between ages 2 and 24 (2). Our studies indicate that, during early stages of digit development, either high androgen or low estrogen activity can lead to a decreased 2D:4D ratio, whereas either low androgen or high estrogen activity can result in an increased 2D:4D ratio. These findings suggest that the digit ratio reflects the balance of androgen to estrogen activity during the digit-forming stages of embryonic development.

Digit 4 Determines 2D:4D Ratio. To determine whether the shift in digit ratios could be attributed to a particular digit, we calculated the digit length index (digit length/tibia length, which controls for systemic effects on skeletal growth) for 2D and 4D after each treatment. Surprisingly, the 2D length index showed no significant response to augmentation with DHT ($P =$ 0.066) or estradiol ($P =$ 0.716) or to antagonism of AR ($P =$ 0.58) or ER ($P =$ 0.257; Fig. 3*D*). By contrast, the 4D length index increased in females exposed to DHT ($P =$ 0.03) or fulvestrant ($P =$ 0.009) and deceased in males exposed to estradiol ($P =$ 0.017) or flutamide ($P =$ 0.012; Fig. 3*D*). Differential growth of 4D, therefore, could account for the sexual dimorphism of the 2D:4D ratio.

To further refine the developmental basis of the 2D:4D ratio, we investigated whether modulation of 4D length by sex hormones could be narrowed down to a specific phalanx (finger bone). Comparison of the proximal and middle phalangeal length index (phalanx length/tibia length) in each treatment group showed that flutamide shortens the proximal and middle phalanges ($P =$ 0.016 and 0.042, respectively), whereas fulvestrant elongated the middle phalanx ($P =$ 0.008) but had no effect on the proximal phalanx ($P =$ 0.269; Fig. 3 *E* and *F*). DHT elongated the middle phalanx ($P =$ 0.015) but had no detectable effect on proximal phalangeal length ($P =$ 0.554; Fig. 3 *E* and *F*). Estradiol, conversely, shortened the proximal phalanx ($P =$ 0.031) but had no effect on the middle phalanx ($P =$ 0.094; Fig. 3 *E* and *F*). Thus, either decreased androgen or increased estrogen activity can cause reduction of phalangeal length, whereas increased androgen or decreased estrogen signaling leads to increased phalangeal length. The phalanx-specific effects of sex steroids suggest that the 2D:4D ratio reflects the totality of changes to the lengths of individual phalanges. These results further support the hypothesis
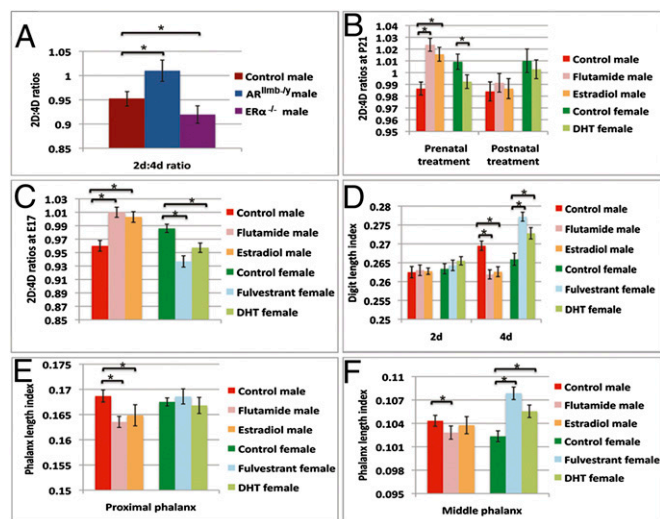
Fig. 3. Experimental manipulation of prenatal androgen and estrogen signaling alters 2D:4D ratios via digit- and phalanx-specific growth. (*A*) 2D:4D ratios in right hindlimbs of AR (*n* = 6) and ER-α (*n* = 7) mutant mice at P0. Control males (*n* = 12) were derived from the same litters as mutants. (*B*) 2D:4D ratios in mice treated with flutamide (anti-AR), fulvestrant (anti-ER), DHT, or estradiol. Digits were measured at P21. All prenatal treatments were done from E12.5 to 15.5, except for fulvestrant, which was administered at E12.5 and 14.5 to avoid labor induction. Postnatal treatment was done from P0 to 3. (*C*) 2D:4D ratios of E17 mouse embryos treated prenatally from E12.5 to 15.5. (*D*) Digit length index (digit length/tibia length) of E17 mouse embryos treated prenatally from E12.5 to 15.5. The 2D index shows no significant response. (*E* and *F*) Phalangeal length index (phalanx length/tibia length) for 4D proximal (*E*) and middle (*F*) phalanges. (*E*) The male proximal phalanx index of 4D is shortened by flutamide or estradiol treatment. The female proximal phalanx index is not significantly altered by fulvestrant or DHT treatment. (*F*) The male middle phalanx index of 4D is shortened by flutamide treatment, and the female middle phalanx index is lengthened by fulvestrant or DHT treatment. Error bars show ± SEM. **P* < 0.05.

that the ratio of androgen to estrogen signaling determines the length of 4D and, ultimately, affects the 2D:4D ratio.

Sex Steroids Regulate Cell Proliferation in Developing Phalanges. Our analysis of the ontogeny of the 2D:4D ratio revealed that sexual dimorphism appears as early as E17 (Fig. 1 *F* and *G*), shortly after the beginning of chondrocyte hypertrophy in developing digits. This finding raised the possibility that sexually dimorphic digit proportions may result from differential control of chondrocyte proliferation by AR and ER-α. To identify the cellular mechanism by which AR and ER-α regulate digit length, we first calculated the mitotic indices of the developing digits using BrdU labeling at E16. Given that the most pronounced changes in digit length were observed in 4D, we focused our analysis on these specific phalanges. In the proximal phalanges of control males, BrdU-positive cells were slightly (but not significantly) more abundant in 4D than in 2D (*P* = 0.054; Fig. 4 *A, B,* and *E*). Antagonism of AR with flutamide had a significantly greater effect on 4D than on 2D (*P* = 0.006), causing a 40% reduction in cell proliferation in 4D, but only a 20% reduction in 2D (Fig. 4 *C* and *D*). This decrease in proliferation can account for the marked reduction in 4D growth and, consequently, the increased 2D:4D ratios in flutamide-treated males. Consistent with these results, when androgen activity was increased by DHT treatment, cell proliferation was enhanced more in 4D than in 2D (*P* = 0.021; Fig. S5).

In control females, the number of BrdU-positive cells was not significantly different between the middle phalanges of 2D and 4D (*P* = 0.158; Fig. 4 *F, G,* and *J*). Antagonism of ER by fulvestrant caused cell proliferation to be significantly higher in 4D relative to 2D (*P* = 0.003; Fig. 4*J*). Fulvestrant led to a 35% increase in the
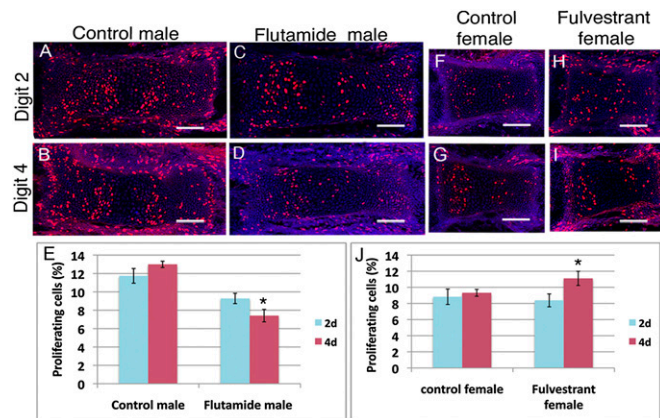
Fig. 4. AR and ER have digit-specific effects on cell proliferation. (*A–D* and *F–I*) BrdU immunolocalization (red) and DAPI staining (blue) of longitudinal sections through proximal and middle phalanges of 2D and 4D of right hindlimbs at E16. Phalanges are oriented with proximal to the left. (Scale bars: 50 μm.) (*E* and *J*) Mitotic indices calculated from sections as represented in *A–D* and *F–I* (*n* = 4 embryos per group) show that antiandrogen treatment (flutamide) decreases cell proliferation in 4D of males (*E*), whereas antiestrogen treatment (fulvestrant) increases cell proliferation in 4D of females (*J*). Error bars show ± SEM. **P* < 0.05.

number of BrdU-positive cells in the middle phalanx of 4D, but only a 0.2% increase in 2D (Fig. 4 *H–J*). Comparison of cell death by using Lysotracker red staining showed no differences in apoptosis between control and flutamide-treated digits (Fig. S6). Thus, the decreased 2D:4D ratio in fulvestrant-treated females is due to increased cell proliferation in the middle phalanx of 4D.

Digit-Specific Regulation of Gene Expression by AR and ER. Based on the finding that androgen and estrogen signaling control sexually dimorphic digit development by governing cell proliferation in specific digits (and even specific phalanges), and the observation that 2D and 4D show differences in AR and ER activity, we tested the hypothesis that the chondrogenic gene network may be regulated differentially in 2D and 4D. Expression of 90 genes known to be involved in skeletal development was compared in 2D and 4D after flutamide and fulvestrant treatments. Quantification of the transcript levels in 4D relative to 2D identified 19 genes with significant, digit-specific responses to either flutamide or fulvestrant (Fig. 5 and Table S1). In males, antagonism of AR with flutamide significantly decreased the relative expression of *Ihh, FgfR2, Sox9, Col10a1, Col4a2,* and *Col12a1,* but increased expression of *Bmp6, Smad3, Wnt5a, Igfbp2, Igfbp5, Runx2, Mmp9,* and *Itgam* (Fig. 5 and Table S1). In females, by contrast, antagonism of ER with fulvestrant significantly increased the relative expression of *Ihh, Col4a2, Col5a1, Col6a2,* and *Col14a1,* but decreased *Fgf3, Msx1, Igfbp2,* and *Igfbp5* (Fig. 5 and Table S1). In no case did flutamide and fulvestrant induce significant changes in the same direction, suggesting that androgen and estrogen have opposite effects on the expression of skeletogenic genes during digit development. Together, our studies indicate that the 2D:4D ratio reflects the effects of prenatal sex steroids on genes that regulate chondrocyte progenitor cell proliferation and differentiation in 4D.

Discussion

The 2D:4D ratio has been proposed to reflect prenatal testosterone exposure; however, this model has been based on correlational studies in humans (3, 11), and, until now, it had not been tested experimentally. Our analysis of mouse digit ratios revealed a significant difference between the male and female 2D:4D ratio as early as E17, and we provide direct evidence that sexually dimorphic digit ratios are caused by androgen and estrogen signaling. We found that 4D has higher levels of AR and ER than 2D and that activity of these receptors influences the 2D:4D ratio by modulating levels of skeletogenic gene expression and cell pro-
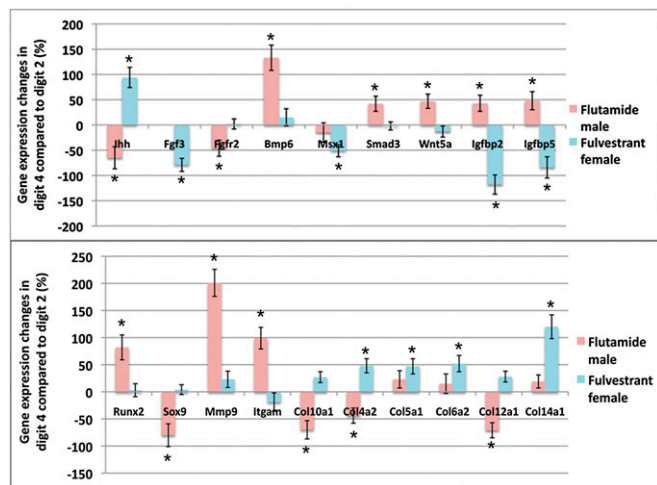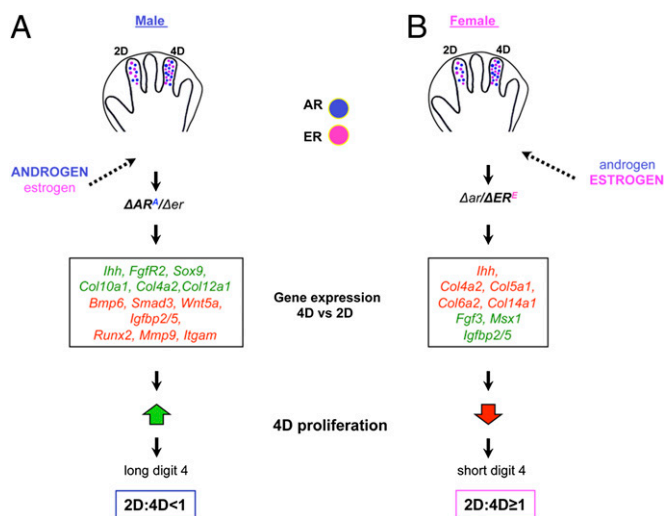
Fig. 5. AR and ER have digit-specific effects on expression of skeletogenic genes. Results of quantitative RT-PCR expression analysis of 90 skeletogenic genes in 2D and 4D are shown. Graphs show relative transcript levels in primordia of 4D compared with 2D, which was assigned a value of 0. The 19 genes showing statistically significant differences ($P < 0.05$) of >40% are shown. See Table S1 for results of all 90 genes. Error bars show ± SEM, and asterisks denote significant differences.

Fig. 6. Developmental basis for the sexually dimorphic 2D:4D ratio. Models for the development of sexually dimorphic digit proportions are shown. AR (blue circles) and ER (pink circles) are present in the digit condensations of male and female embryos, with higher levels found in 4D. (A) In males, digits are exposed to high levels of circulating androgen and low levels of circulating estrogen, which results in preferential binding and activation of AR (AR[A] represents the androgen bound to the AR). High AR activity and low ER activity (ΔAR[A]/Δer) in males leads to differential gene expression profiles in 4D relative to 2D (green indicates genes higher in 4D, and red indicates genes higher in 2D). In turn, chondrocyte proliferation is increased in the proximal phalanx of 4D, which results in elongation of 4D relative to 2D, leading to a lower 2D:4D ratio. (B) In females, digits are exposed to high levels of estrogen and low levels of androgen, leading to preferential binding and activation of ER (ER[E]). Low AR activity and high ER activity (Δar/ΔER[E]) induces an opposite shift in the skeletogenic gene expression profile of 4D relative to 2D (indicated by gene names in green and red, as above). Higher levels of activated ER cause decreased chondrocyte proliferation in the middle phalanx of 4D, which reduces its growth relative to 2D and results in a higher 2D:4D ratio.

liferation in a digit-specific manner. We propose that polarized distribution of AR and ER-α in digit primordia, which is conserved between the sexes, together with sex-specific profiles of circulating hormones result in differential activation of hormone receptors in 2D and 4D. In turn, AR and ER-α differentially regulate expression of chondrogenic genes in D4, which underlies differential growth of digits in males and females (Fig. 6).

Our finding that the 2D:4D ratios detected at E17 are not significantly different from those found in 3-wk-old weanlings or in adults suggests that sexually dimorphic digit development occurs during a short time window of prenatal development and that these differences persist over the life of the animal. The difference in scale between mouse and human digit ratios, along with differences among mouse strains, might explain the variable results of previous studies of rodent digit ratios (12, 14, 24, 25). The dimorphism of 2D:4D ratios between male and female mice examined by us (this study) and by others (12) is considerably less pronounced than that reported for humans. The weaker dimorphism of mouse digit ratios could reflect hormone transfer between male and female embryos in the mouse uterine horns (26). Indeed, studies of human dizygotic twins have shown that females with a male twin have lower 2D:4D ratios than same-sex female twins (27). When we modulated AR or ER activity experimentally in mice, the differences in digit ratios became significantly more pronounced and approached the ratios found in humans. These results are consistent with reports that humans with AR mutations that affect the response to androgens, including complete androgen insensitivity syndrome, have associated changes in their 2D:4D ratios (28, 29).

In adults, the role of ER in skeletal homeostasis is well known (30). This study implicates androgen and estrogen in development of the early cartilaginous skeleton. Our gene expression data show that sex steroids control digit development through regulation of at least 19 members of the skeletogenic gene network. We found quantitative differences in their expression levels in 2D and 4D, indicating that there is a molecular 2D:4D difference during early digit development, before sexually dimorphic growth occurs. Interestingly, several of these genes have been shown to be regulated by steroids in skeletal and other tissues (31–34), and genetic studies have shown that *Wnt5a, Ihh, Bmp6, Fgfr2, lgfbp2/5, Sox9,* and *Runx2* all play important roles in digit development (35–37). For example, *Wnt5a* has been shown to regulate the pace of chondrocyte proliferation and maturation in long bones (38). Our findings indicate that AR is a negative regulator of *Wnt5a* ex-

pression in digits and that the up-regulation of *Wnt5a* in 4D after antagonism of AR may underlie the reduction of cell proliferation and shortening of this digit in males that develop increased/feminized 2D:4D ratios.

It is interesting that the stages at which phalangeal growth can be influenced by AR and ER are also the stages when sex steroids masculinize and feminize the brain (39). Strong correlations exist between 2D:4D ratios and a suite of behavioral phenotypes, fertility, diseases, athleticism, and sexual orientation (5, 7–9, 11, 40, 41). Evolutionarily, hormonal regulation of sexually dimorphic brain development, a likely target of selection, may have had secondary effects on structures such as the digits. Digit ratios, therefore, may be simply readouts of androgen to estrogen activity during this developmental period. In light of this hypothesis, it is intriguing that several genes identified in our study also have roles in development of the brain (42, 43) and other sexually dimorphic structures such as genitalia, mammary glands, and hair (44, 45). This finding raises the possibility that the same developmental control genes might mediate localized, organ-specific responses to systemically circulating hormones. Lastly, it is noteworthy that male mice with diminished AR function and increased/feminized digit ratios also developed hypospadias, a urethral tube defect that can present as feminization of the genitalia. Thus, analysis of digit ratios in the hypospadias patient population could be an informative indicator of perturbed hormonal signaling during embryonic development.

Methods

Animals and Digit Length Measurements. *AR[flox]* mice were kindly provided by Guido Verhoeven (Katholieke Universiteit Leuven) via Marvin Maestrich and Connie Wang (University of Texas M. D. Anderson Cancer Center). *Prx1[Cre]*

and ER-α knockout mice were purchased from Jax. Double-blind linear measurements of the proximal and middle phalanges of 2D and 4D in skeletal preparations of CD-1 mice were made by using a calibrated eyepiece reticule on a stereo dissecting microscope (46). Stage of copulatory plug was designated E0.5 (CD1 mice are born at E19–20). Details of flutamide, fulvestrant, DHT, and estradiol treatments are described in *SI Methods*.

In Situ Hybridization, Cell Death, Cell Proliferation, and Skeletal Preparation. RNA whole-mount in situ hybridization, Lysotracker red (Molecular Probes) staining, and skeletal preparations were performed as described (47). *Sox9* plasmid was kindly provided by Peter Koopman (University of Queensland, St. Lucia, Australia). For cell proliferation analysis, BrdU (100 mg/kg) was injected 24 h after treatment with steroid or steroid receptor inhibitor, and embryos were collected 2 h later for immunohistochemistry.

Immunohistochemistry of AR and ER-α. Immunohistochemistry was performed by using rabbit anti-AR and anti-ER-α primary antibodies (Santa Cruz) diluted 1:200 and incubated overnight at 4 °C. Antibodies were detected by using the TSA kit (Invitrogen) according to the manufacturer's protocol visualized on a Leica TSM Sp5 confocal microscope.

Quantitative RT-PCR. Quantitative RT-PCR was modified from a published method (47). Digits 2 and 4 were dissected from staged CD1 mouse embryos and were pooled by digit number and treatment. Skeletogenic gene expression was determined by using the Osteogenesis PCR array (PAMM-026;

SABiosciences) and the 7900 HT Fast real-time PCR system (Applied Biosystems) according to the manufacturer's protocol. For further details, see *SI Methods* and Table S2.

Estimate of AR, ER-α, and BrdU Positive Cell Numbers. For AR and ER-α immunolabeling, longitudinal sections were cut at 12 μm, and five sections from the midpoint of each sample (n = 4) were selected to ensure we captured the digit. Starting from mesenchyme/epithelium border, five counting squares (100 × 50 μm²) were placed 10 μm apart on both 2D and 4D in E12.5 limbs. For E14.5 limb, six counting squares (100 × 50 μm²) were placed 20 μm apart on both 2D and 4D of each sample (n = 4). For BrdU analysis, BrdU-positive cells and total cells (visualized by DAPI) were counted in sections through each phalanx, and five sections from the midpoint of each sample (n = 3) were selected for measurements.

Statistical Analysis. All group differences in our dependent variables were revealed by using two-tailed Student's t tests with α-level set at 0.05, and all effect sizes (Cohen's d) were >0.8.

1. Baker F (1888) Anthropological notes on the human hand. *Am Anthropol* 1:51–76.
2. Manning JT, Scutt D, Wilson J, Lewis-Jones DI (1998) The ratio of 2nd to 4th digit length: A predictor of sperm numbers and concentrations of testosterone, luteinizing hormone and oestrogen. *Hum Reprod* 13:3000–3004.
3. Breedlove SM (2010) Organizational hypothesis: Instances of the fingerpost. *Endocrinology* 151:4116–4122.
4. Manning JT, et al. (2000) The 2nd:4th digit ratio, sexual dimorphism, population differences, and reproductive success. Evidence for sexually antagonistic genes? *Evol Hum Behav* 21:163–183.
5. Manning JT, Taylor RP (2001) Second to fourth digit ratio and male ability in sport: Implications for sexual selection in humans. *Evol Hum Behav* 22:61–69.
6. Manning JT, Bundred PE (2000) The ratio of 2nd to 4th digit length: A new predictor of disease predisposition? *Med Hypotheses* 54:855–857.
7. Manning JT, Baron-Cohen S, Wheelwright S, Sanders G (2001) The 2nd to 4th digit ratio and autism. *Dev Med Child Neurol* 43:160–164.
8. Coates JM, Gurnell M, Rustichini A (2009) Second-to-fourth digit ratio predicts success among high-frequency financial traders. *Proc Natl Acad Sci USA* 106:623–628.
9. Williams TJ, et al. (2000) Finger-length ratios and sexual orientation. *Nature* 404: 455–456.
10. Hönekopp J, Bartholdt L, Beier L, Liebert A (2007) Second to fourth digit length ratio (2D:4D) and adult sex hormone levels: New data and a meta-analytic review. *Psychoneuroendocrinology* 32:313–321.
11. Manning JT (2002) *Digit Ratio: A Pointer to Fertility, Behavior, and Health* (Rutgers University Press, Piscataway, NJ) 1st Ed.
12. Brown WM, Finn CJ, Breedlove SM (2002) Sexual dimorphism in digit-length ratios of laboratory mice. *Anat Rec* 267:231–234.
13. Manno FA, 3rd (2008) Measurement of the digit lengths and the anogenital distance in mice. *Physiol Behav* 93:364–368.
14. Bailey AA, Wahlsten D, Hurd PL (2005) Digit ratio (2D:4D) and behavioral differences between inbred mouse strains. *Genes Brain Behav* 4:318–323.
15. Manning JT, Callow M, Bundred PE (2003) Finger and toe ratios in humans and mice: Implications for the aetiology of diseases influenced by HOX genes. *Med Hypotheses* 60:340–343.
16. Tyagi RK, et al. (2000) Dynamics of intracellular movement and nucleocytoplasmic recycling of the ligand-activated androgen receptor in living cells. *Mol Endocrinol* 14: 1162–1174.
17. Yamashita S (1998) Localization and functions of steroid hormone receptors. *Histol Histopathol* 13:255–270.
18. Lutchmaya S, Baron-Cohen S, Raggatt P, Knickmeyer R, Manning JT (2004) 2nd to 4th digit ratios, fetal testosterone and estradiol. *Early Hum Dev* 77:23–28.
19. Zagar Y, Chaumaz G, Lieberherr M (2004) Signaling cross-talk from Gbeta4 subunit to Elk-1 in the rapid action of androgens. *J Biol Chem* 279:2403–2413.
20. Dai Z, et al. (2007) Resveratrol enhances proliferation and osteoblastic differentiation in human mesenchymal stem cells via ER-dependent ERK1/2 activation. *Phytomedicine* 14:806–814.
21. Logan M, et al. (2002) Expression of Cre recombinase in the developing mouse limb bud driven by a Prxl enhancer. *Genesis* 33:77–80.
22. Kontula KK, Seppänen PJ, van Duyne P, Bardin CW, Jänne OA (1985) Effect of a nonsteroidal antiandrogen, flutamide, on androgen receptor dynamics and ornithine decarboxylase gene expression in mouse kidney. *Endocrinology* 116:226–233.
23. Garn SM, Poznanski AK, Larson KE (1975) Magnitude of sex differences in dichotomous ossification sequences of the hand and wrist. *Am J Phys Anthropol* 42:85–89.
24. Hurd PL, et al. (2008) Intrauterine position effects on anogenital distance and digit ratio in male and female mice. *Arch Sex Behav* 37:9–18.
25. Talarovicová A, Krsková L, Blazeková J (2009) Testosterone enhancement during pregnancy influences the 2D:4D ratio and open field motor activity of rat siblings in adulthood. *Horm Behav* 55:235–239.
26. Hauser H, Gandelman R (1983) Contiguity to males in utero affects avoidance responding in adult female mice. *Science* 220:437–438.
27. van Anders SM, Vernon PA, Wilbur CJ (2006) Finger-length ratios show evidence of prenatal hormone-transfer between opposite-sex twins. *Horm Behav* 49:315–319.
28. Manning JT, Bundred PE, Newton DJ, Flanagan BF (2003) The second to fourth digit ratio and variation in the androgen receptor gene. *Evol Hum Behav* 24:399–405.
29. Berenbaum SA, Bryk KK, Nowak N, Quigley CA, Moffat S (2009) Fingers as a marker of prenatal androgen exposure. *Endocrinology* 150:5119–5124.
30. Weitzmann MN, Pacifici R (2006) Estrogen deficiency and bone loss: An inflammatory tale. *J Clin Invest* 116:1186–1194.
31. Katayama S, et al. (2006) The expression of Hedgehog genes (Ihh, Dhh) and Hedgehog target genes (Ptc1, Gli1, Coup-TfII) is affected by estrogenic stimuli in the uterus of immature female rats. *Toxicol Appl Pharmacol* 217:375–383.
32. Ngamniyom A, Magtoon W, Nagahama Y, Sasayama Y (2009) Expression levels of hormone receptors and bone morphogenic protein in fins of medaka. *Zoolog Sci* 26:74–79.
33. McCarthy TL, Chang WZ, Liu Y, Centrella M (2003) Runx2 integrates estrogen activity in osteoblasts. *J Biol Chem* 278:43121–43129.
34. Nemeth MJ, Topol L, Anderson SM, Yang Y, Bodine DM (2007) Wnt5a inhibits canonical Wnt signaling in hematopoietic stem cells and enhances repopulation. *Proc Natl Acad Sci USA* 104:15436–15441.
35. Fisher MC, Meyer C, Garber G, Dealy CN (2005) Role of IGFBP2, IGF-I and IGF-II in regulating long bone growth. *Bone* 37:741–750.
36. Wan M, Cao X (2005) BMP signaling in skeletal development. *Biochem Biophys Res Commun* 328:651–657.
37. Zhou J, et al. (2007) IHH and FGF8 coregulate elongation of digit primordia. *Biochem Biophys Res Commun* 363:513–518.
38. Yang Y, Topol L, Lee H, Wu J (2003) Wnt5a and Wnt5b exhibit distinct activities in coordinating chondrocyte proliferation and differentiation. *Development* 130:1003–1015.
39. Knoll JG, Wolfe CA, Tobet SA (2007) Estrogen modulates neuronal movements within the developing preoptic area-anterior hypothalamus. *Eur J Neurosci* 26:1091–1099.
40. Manning JT, Churchill AJ, Peters M (2007) The effects of sex, ethnicity, and sexual orientation on self-measured digit ratio (2D:4D). *Arch Sex Behav* 36:223–233.
41. Robinson SJ, Manning JT (2000) The ratio of 2nd to 4th digit length and male homosexuality. *Evol Hum Behav* 21:333–345.
42. Furuta Y, Piston DW, Hogan BL (1997) Bone morphogenetic proteins (BMPs) as regulators of dorsal forebrain development. *Development* 124:2203–2212.
43. Andersson ER, et al. (2008) Wnt5a regulates ventral midbrain morphogenesis and the development of A9-A10 dopaminergic cells in vivo. *PLoS ONE* 3:e3517.
44. Eblaghie MC, et al. (2004) Interactions between FGF and Wnt signals and Tbx3 gene expression in mammary gland initiation in mouse embryos. *J Anat* 205:1–13.
45. Cohn MJ (2011) Development of the external genitalia: Conserved and divergent mechanisms of appendage patterning. *Dev Dyn* 240:1108–1115.
46. Karp SJ, et al. (2000) Indian hedgehog coordinates endochondral bone growth and morphogenesis via parathyroid hormone related-protein-dependent and -independent pathways. *Development* 127:543–548.
47. Seifert AW, Zheng Z, Ormerod BK, Cohn MJ (2010) Sonic hedgehog controls growth of external genitalia by regulating cell cycle kinetics. *Nat Commun*, 10.1038/1020.

Supporting Information

Zheng and Cohn 10.1073/pnas.1108312108

SI Methods

Animals and Treatments. Flutamide (120 mg/kg, 40 mg/mL, dissolved in corn oil with 1% ethanol), fulvestrant (1 mg/kg, 50 mg/mL, dissolved in ethanol and diluted 100 times in corn oil), DHT (2 mg/kg, 100 mg/mL, dissolved in ethanol diluted 100 times in corn oil), estradiol (300 μg/kg, 15 mg/mL dissolved in ethanol and diluted 100 times in corn oil), or corn oil control vehicle (corn oil with 1% ethanol) was administered by oral gavage (flutamide) or IP injection (DHT, estradiol, fulvestrant) of pregnant females from E12.5 to E15.5 once daily, except for fulvestrant which was administered at E12.5 and E14.5 to prevent induction of labor. The effect of treatment on embryos was validated by measurements of anogenital distance (Fig. S7A). Anogenital distance is a confirmed sexually dimorphic marker in rodents, is permanently affected by prenatal androgen exposure (1, 2), and is obvious as early as E15.5 (Fig. S7B). Sample sizes for pharmacological treatment groups (Fig. 3 and Figs. S3, S4, and S7) range from a minimum of $n = 15$ to a maximum of $n = 23$. Wild-type sample sizes are provided in the figure legends. All animal experiments were performed in accordance with institutional guidelines.

Quantitative RT-PCR. Total RNA was extracted from 2D and 4D by using RNeasy plus micro kit (Qiagen), and RNA quantity (>100 ng/μL) and purity (260/280 > 2.0, 260/230 > 1.65) were determined by using a Nanodrop. RNA integrity (RIN > 8.5) and 28S/18S ratio (>1.5) were assessed by using a Bioanalyzer 2100 (Agilent Technologies). A quantity of 500 ng of high-quality RNA for each pooled sample ($n = 3$) was converted into cDNA by using the RT^2 First Strand cDNA Kit (SABiosciences). Skeletogenic gene expression was determined by using the Osteogenesis PCR Array (PAMM-026; SABiosciences) and the 7900 HT Fast Real-Time PCR system (Applied Biosystems) according to the manufacturer's protocol. The complete list of genes assayed on the array can be found at the manufacturer's Web site. For other genes, expression was detected by using the CFX96 Real Time system (Bio-Rad) and QPCR system (Bio-Rad) with Actb (3) and Gapdh (4) as controls. Primers not previously published were designed by using Beacon Designer Software, except for Hoxa13, which was purchased from SA-Biosciences. The qRT-PCR primers designed for this study are listed in Table S2. The Web-Based PCR Array Data Analysis system (SABiosciences) was used to analyze PCR array results, and results of qRT-PCR assays not represented on the array were determined using ΔΔCt method (5).

1. Hotchkiss AK, et al. (2007) Prenatal testosterone exposure permanently masculinizes anogenital distance, nipple development, and reproductive tract morphology in female Sprague-Dawley rats. *Toxicol Sci* 96:335−345.
2. Manno FA, 3rd (2008) Measurement of the digit lengths and the anogenital distance in mice. *Physiol Behav* 93:364−368.
3. Seifert AW, Zheng Z, Ormerod BK, Cohn MJ (2010) Sonic hedgehog controls growth of external genitalia by regulating cell cycle kinetics. *Nat Commun* 1:23.
4. Crusselle-Davis VJ, Vieira KF, Zhou Z, Anantharaman A, Bungert J (2006) Antagonistic regulation of beta-globin gene expression by helix-loop-helix proteins USF and TFII-I. *Mol Cell Biol* 26:6832−6843.
5. Pfaffl MW (2001) A new mathematical model for relative quantification in real-time RT-PCR. *Nucleic Acids Res* 29:e45.
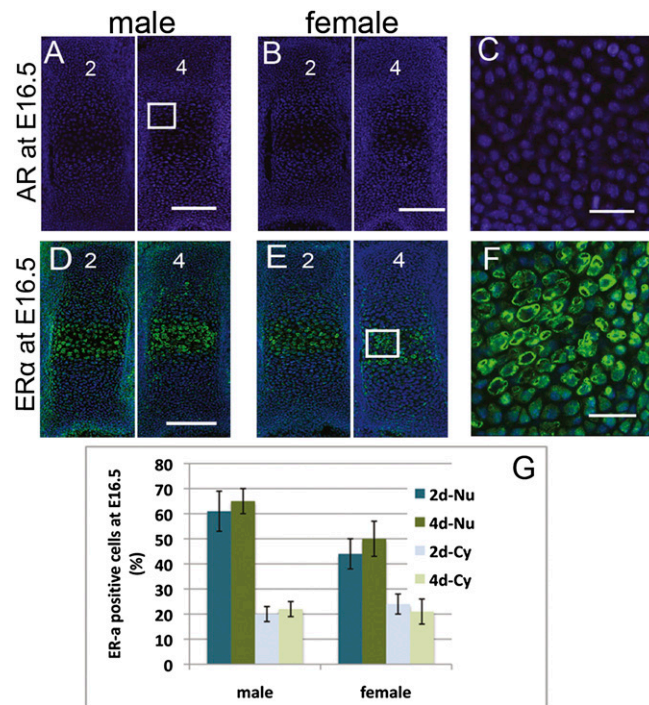
Fig. S1. AR and ER-α localization in 2D and D4 in E16.5 CD-1 mice. (*A, B, D,* and *E)* Longitudinal sections through proximal phalanges stained with DAPI (blue) and antibodies against AR (red, which is undetectable in *A* and *B*) and ER-α (green in *D* and *E*). D2 and 4D are numbered. White boxes in *A* and *E* are enlarged in *C* and *F*. (Scale bars: 50 μm in *A, B, D,* and *E*; 10 μm in *C* and *F*.) (*G*) Quantitative analysis of ER-α–positive cells in E16.5 proximal phalanges with nuclear (Nu) and cytoplasmic (Cy) staining. AR staining at this stage was below detectable levels. Error bars show ± SEM.
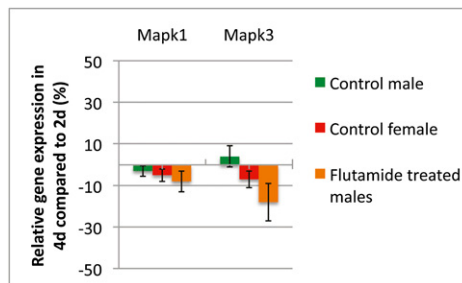

Fig. S2. Quantitative RT-PCR expression analysis of *Mapk1* and *Mapk3* in 2D and 4D. Graphs show relative transcript levels in 4D compared with 2D. Note that there is no significant difference between 2D and 4D. Error bars show ± SEM.
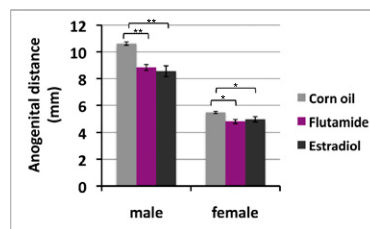
Fig. S3. Postnatal antiandrogen or estradiol treatment reduces anogenital distance in mice. Anogenital distance was measured at P21 following daily treatments from P0 to P3 with flutamide (120 mg/kg) and estradiol (300 μg/kg). The results show that either flutamide ($P = 0.001$) or estradiol ($P = 0.005$) can significantly reduce anogenital distance during postnatal growth and development. Digit ratios are not affected by treatments at these stages.
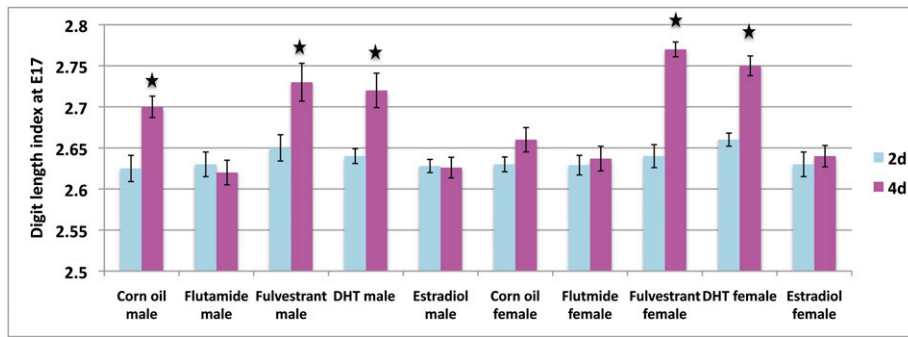
Fig. S4. Modulation of prenatal androgen and estrogen signaling alters 4D length in both males and females. All treatments were done prenatally, from E12.5 to 15.5, except for fulvestrant, which was administered at E12.5 and 14.5 to avoid labor induction. Digit length index was calculated by dividing digit length by tibia length to control for systemic changes in skeletal growth. Error bars show ± SEM. *P < 0.05.
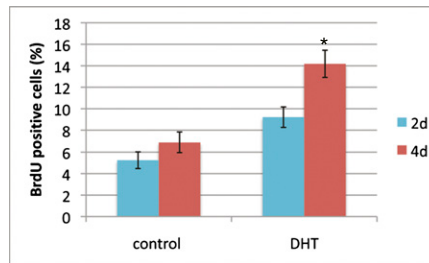
Fig. S5. Effects of DHT treatment on cell proliferation in 2D and 4D. Mitotic indices, calculated from longitudinal sections through 2D and 4D, show that DHT significantly increases cell proliferation in 4D relative to 2D. Error bars show ± SEM. *P < 0.05.

Control male   Flutamide male
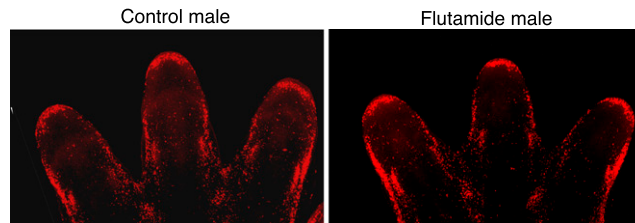
Fig. S6. Comparison of cell death in the digits of control (*Left*) and flutamide-treated (*Right*) male mice at E14.5. Lysotracker red staining showed no obvious differences in apoptosis between control and flutamide-treated digits 24 h after treatment.
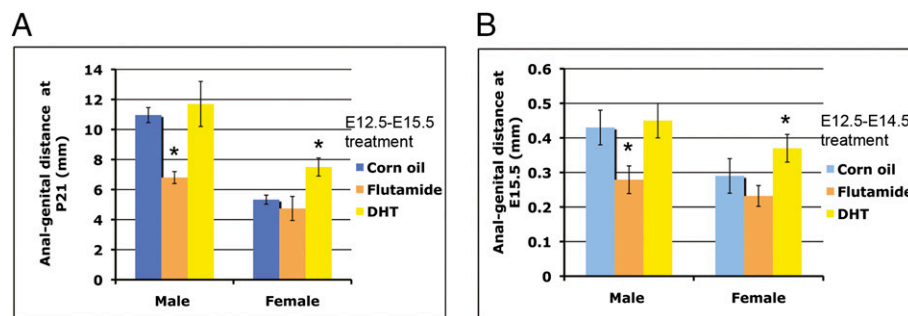
Fig. S7. Effects of prenatal flutamide and DHT treatment on anogenital distance. (*A*) Prenatal administration of flutamide (120 mg/kg from E12.5 to 15.5, once daily) significantly reduces (P < 0.001) anogenital distance in male mice at P21. DHT treatment (2 mg/kg from E12.5 to 15.5, once daily) significantly increases (P = 0.007) the anogenital distance in female mice at P21. (*B*) Anogenital distance is affected as early as E15.5 following treatment with flutamide (P = 0.012) or DHT (P = 0.027) between stages E12.5 and 14.5.

Table S1. Relative gene expression in 4D compared with 2D after flutamide and fulvestrant treatment

Gene	Flutamide treatment		Fulvestrant treatment	
	P*	Fold change[†]	P*	Fold change[†]
Ahsg	NA	NA	NA	NA
Alpl	0.399206	1.48	0.266898	1.37
Ambn	0.963548	1.02	0.817367	1.01
Anxa5	0.026445	1.36	0.363989	1.16
Bgn	0.393466	1.12	0.57909	−1.05
Bmp1	0.005414	1.15	0.899569	1.02
Bmp2	0.059722	1.33	0.078897	1.11
Bmp3	0.444235	1.14	0.670644	−1.04
Bmp4	0.306083	−1.07	0.913614	−1.01
Bmp5	0.749093	−1.04	0.882607	−1.04
Bmp6	0.034389	**2.62**	0.171142	1.16
Bmpr1a	0.067409	−1.09	0.62312	−1.06
Bmpr1b	0.948885	−1	0.544714	1.09
Cd36	0.295599	1.77	0.130393	−1.5
Cdh11	0.201374	1.17	0.635321	−1.11
Col10a1	0.018254	**−1.66**	0.393528	1.28
Col11a1	0.264219	1.29	0.608184	−1.43
Col12a1	0.026702	**−1.68**	0.799201	1.33
Col14a1	0.186024	1.19	0.0278857	**2.29**
Col1a1	0.157679	1.5	0.304379	1.18
Col1a2	0.142395	1.26	0.454542	−1.04
Col2a1	0.456362	1.18	0.411452	1.17
Col3a1	0.123003	1.51	0.280583	1.17
Col4a1	0.072995	1.59	0.615775	1.07
Col4a2	0.040047	**−1.44**	0.003599	**1.47**
Col5a1	0.060589	1.28	0.036235	**1.46**
Col6a1	0.053092	1.51	0.19521	1.48
Col6a2	0.052914	1.26	0.017826	**1.51**
Col7a1	0.450404	1.17	0.572001	1.17
Comp	0.8629	−1.01	0.810341	−1.06
Csf2	NA	NA	NA	NA
Csf3	NA	NA	NA	NA
Ctsk	0.054292	2.54	0.389205	−1.75
Dmp1	0.85548	NA	0.501604	NA
Egf	0.566286	−1.46	0.018661	1.29
Enam	NA	NA	NA	NA
Fgf1	0.615475	1.27	0.0302511	1.22
Fgf2	0.625374	1.79	0.715929	−1.03
Fgf3	NA	NA	0.0397	**−1.74**
Fgfr1	0.83189	1.02	0.5264	−1.06
Fgfr2	0.031945	**−1.48**	0.935737	−1.01
Fgfr3	0.10594	1.33	0.327585	−1.26
Flt1	0.305575	1.27	0.934638	−1
Fn1	0.675327	−1.1	0.908728	1.01
Gdf10	0.318849	1.17	0.599319	1.05
Hoxa13	0.028932	1.37	0.041667	−1.27
Icam1	0.40052	1.16	0.460418	−1.19
Igf1	0.652132	1.05	0.0135072	−1.16
Igf1r	0.100419	1.32	0.620577	1.06
Igfbp2	0.034528	**1.46**	0.020395	**−2.39**
Igfbp5	0.041755	**1.49**	0.033681	**−1.85**
Ihh	0.027431	**−1.68**	0.015481	**1.92**
Itga2	0.503951	1.22	0.610009	1.05
Itga2b	0.649112	1.11	0.441788	1.11
Itga3	0.932126	−1.08	0.351632	−1.09
Itgam	0.011399	**2**	0.090589	−1.24
Itgav	0.585689	−1.07	0.960074	−1
Itgb1	0.002062	1.35	0.218512	1.19
Mmp10	0.921681	−1.16	0.901799	1.07
Mmp2	0.026878	1.37	0.178692	1.17

Table S1. Cont.

Gene	Flutamide treatment		Fulvestrant treatment	
	P*	Fold change[†]	P*	Fold change[†]
Mmp8	NA	NA	NA	NA
Mmp9	0.023637	**3.9**	0.20607	1.23
Msx1	0.06553	−1.25	0.007759	**−1.49**
Nfkb1	0.027757	1.17	0.607161	1.03
Pdgfa	0.360583	1.15	0.040907	−1.17
Phex	0.060886	1.79	0.059236	1.81
Runx2	0.034153	**1.77**	0.114711	1.02
Scarb1	0.77894	1.03	0.939359	1.01
Serpinh1	0.682536	1.14	0.862305	−1.02
Smad1	0.540028	1.09	0.54183	−1.08
Smad2	0.073445	2.9	0.0327889	1.13
Smad3	0.048333	**1.45**	0.513535	1.09
Smad4	0.17833	1.21	0.056494	−1.45
Sost	0.633648	−1.12	0.465883	−1.38
Sox9	0.02586	**−1.76**	0.0818246	1.15
Tfip11	0.15807	1.27	0.669522	−1.04
Tgfb1	0.00128	1.19	0.0445893	1.08
Tgfb2	0.644308	1.13	0.129208	1.19
Tgfb3	0.151979	1.33	0.198769	1.15
Tgfbr1	0.026563	1.2	0.764842	1.03
Tgfbr2	0.871591	1.02	0.471603	−1.03
Tgfbr3	0.076085	2.67	0.094265	1.04
Tnf	NA	NA	NA	NA
Tuft1	0.426009	1.21	0.496134	−1.05
Twist1	0.375008	−1.5	0.076953	−1.55
Vcam1	0.057933	1.19	0.366577	−1.09
Vdr	0.116554	1.55	0.899057	−1.08
Vegfa	0.152263	1.9	0.790228	−1.17
Vegfb	0.097637	1.38	0.788172	−1.14
Wnt5a	0.03783	**1.48**	0.17962	−1.18

*Italic type indicates significant ($P < 0.05$) changes in expression levels.
[†]Positive fold change indicates up-regulation in 4D vs. 2D; negative fold change indicates down-regulation in 4D vs. 2D. Fold changes for genes shown in Fig. 4 are in boldface type.

Table S2. Primers designed in this study

Name	Sequences	GenBank accession no.
Igfbp2		NM_008342
For	ATCCCGAACACCAGCAGAAATG	
Rev	GCCCTCCATACCACCCTTCC	
Igfbp5		NM_010518
For	TGCTCACTCCTCTTCTCCTTCC	
Rev	TCTCTTCTCCTTGGCTCACTCC	
Ihh		NM_010544
For	GAGACACCATTGAGACTTGACCAG	
Rev	GTGAAGAATCGCAGCCAGAGC	
Wnt5a		NM_009524
For	AAAGTAGCCTTTCTGCTTCCTGCC	
Rev	TATGTGGTGAGCTGGTTTGCTTCG	
Fgfr3		NM_001163216
For	GCCAGGAGCACCAAACAAGAATG	
Rev	AAGGTAGCAGTGGGAAATGAGAGG	
Mapk1		NM_011949
For	TTGTGGCTTTGGGACTGTGTG	
Rev	GCATATTCATCCGTTACCTTCTTACC	
Mapk3		NM_011952
For	AGGAGCGGCTGAAGGAGTTG	
Rev	GCAGAGAAGGAGCAGGTAGGAG	